Low-Loss Connection of Embedded Optical Fiber Sensors Using a Self-Written Waveguide

Jeroen Missinne, Geert Luyckx, Eli Voet and Geert Van Steenberge

In: IEEE Photonics Technology Letters, Volume 29 (Issue 20), page 1731-1734, 2017.

https://doi.org/10.1109/LPT.2017.2747630

Low-Loss Connection of Embedded Optical Fiber Sensors Using a Self-Written Waveguide

Jeroen Missinne, Geert Luyckx, Eli Voet and Geert Van Steenberge

***Abstract*— This letter reports on a new concept for making a low-loss connection to an optical fiber sensor which is embedded in a fiber reinforced composite material for structural health monitoring. First, a cross-section of the composite is made to reveal the end-face of the embedded optical fiber. Then, an external fiber is aligned and an intermediate polymer-based self-written waveguide (SWW) is fabricated between both fibers. This SWW bridges the gap and serves as mode size converter ensuring a low-loss optical connection even if both fibers have dissimilar mode field diameters. The advantage of this approach is that no special care needs to be taken during the composite production cycle not to damage the sensor fiber in- or egress points, since it will be reconnected afterwards.**

***Index Terms*—Bragg gratings, composite materials, connectors, optical fibers.**

I. Introduction

COMPOSITE materials are widely used in applications requiring high-strength and light-weight materials such as in airplanes, wind turbine blades, high pressure vessels etc. Measuring in-situ material deformations and monitoring the integrity of these composites can be performed using optical fiber sensors [1, 2]. Ideally, those sensing fibers are embedded inside the composite material where they are also protected from the harsh environment. The potential of this sensing technology is clear, but adoption by industry is currently slowed down by the lack of flexible connection strategies of these embedded optical fibers. Indeed, the weakest point of this sensor system is where the fiber enters the composite host material: the so-called 'in- or egress point'. To deal with this issue, a number of methods are currently used, but these are not fully compatible with composite manufacturing techniques, involve high optical losses, and moreover, once a fiber fractures at the egress points, it cannot be repaired.

The strategies mainly used are either based on protecting the entry point of the optical fiber during composite fabrication (e.g. using tubing) [3], or based on incorporating a discrete optical connector at the composite edge [4, 5]. The first approach does not allow any repair if the fiber breaks at the entry point and often requires an adaptation of the composite production mold to lead out the fiber. The second approach is not desired from a mechanical point of view because of undesired distortion of the composite at the location of the connector and requires adaptation of the production process to ensure the accurate placement of the connector. It is clear that both approaches do not allow trimming of the composite edges after fabrication due to the presence of the fiber or the connector, which is a huge disadvantage. Furthermore, the sensing fibers may be different than the standard single mode telecom fibers (ITU-T G.652) for which a lot of optical instrumentation equipment is optimized.

Manuscript submitted May 30, 2017. This work was supported by the European Space Agency (ESA), under contract nr. 4000114365/15/NL/CBi/GM.

J. Missinne and G. Van Steenberge are with the CMST, Ghent-University & imec, Ghent, Belgium. (e-mail: jeroen.missinne@ugent.be; geert.vansteenberge@ugent.be).

G. Luyckx and E. Voet are with Com&Sens BVBA, Ghent, Belgium (email: gluyckx@com-sens.eu; evoet@com-sens.eu).

II. Connection concept and methods

To tackle the above-mentioned challenges, a novel concept is described in this letter which is based on a low-loss optical 'splice', which is packaged to ensure mechanical robustness. The technique does not require changes to the composite production process: after production, the embedded fiber is exposed by making a cross-sectional cut, the external fiber is aligned with it and then a direct optical splice is made. As illustrated in Fig. 1, the optical splice is implemented using an intermediate Self-Written Waveguide (SWW) between both pre-aligned fibers. Such an SWW is formed when UV-light is launched through a fiber which is immersed in an appropriate UV-curable polymer resin. Due to the increase in refractive index of the resin upon polymerization (which starts at the tip of the fiber where the optical power density is the highest), a lens-like structure is formed. This causes an increased light intensity at the lens front leading to a progressively growing polymerized region forming a waveguide structure [6]. In this case, the UV-light is launched through the external fiber and therefore, the SWW serves as an extension waveguide, which is self-aligned to this fiber. It will be shown that such an intermediate SWW can act as a mode size converter allowing low connection losses between an embedded sensor fiber and a standard single mode fiber which may have a different numerical aperture (NA) and different mode field diameter (MFD). The fiber sensors investigated in this work are Draw Tower fiber Bragg Grating sensors (DTG® technology, from FBGS International), i.e. fibers which have the Bragg grating sensors inscribed during the fiber drawing process, as such keeping the pristine fiber breaking strength. These DTG fibers

differ from standard telecom fibers, i.e. they have a numerical aperture (NA) of 0.26 compared to 0.13 for a standard ITU-T G.652 fiber. Therefore, direct coupling of both fibers leads to losses due to a mismatch in MFD. These DTG fibers measure 125 µm in diameter and have an Ormocer® coating yielding a total diameter of 195 µm.

The process described herein is optimized for fiber sensors operating around 1550 nm which have been embedded either in glass fiber reinforced polymer (GFRP) or carbon fiber reinforced polymer (CFRP) composites.

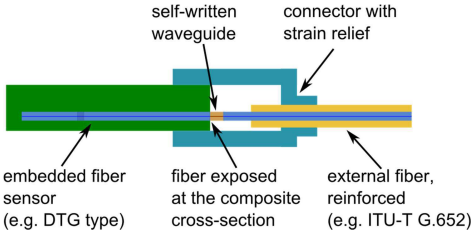

Fig. 1. Concept of the technology for making an edge connection between an external standard single mode fiber (ITU-T G.652) and an embedded fiber with Draw Tower Grating (DTG) sensors by employing an intermediate self-written waveguide.

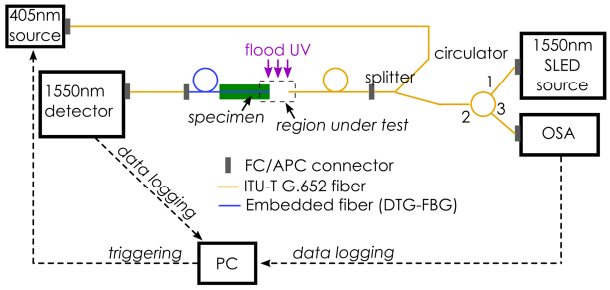

Fig. 2. Setup used for fabricating SWW optical connections with simultaneous insertion loss monitoring.

The procedure for making the optical connection is as follows. First, the sensor fiber (DTG type) is embedded during the composite production cycle without a need to protect the egress point. Secondly, a cut is made (e.g. using a diamond blade or waterjet) which is subsequently locally polished (using type P2400 and P4000 abrasive papers), revealing the end-face of the embedded fiber. Then, the external fiber (ITU-T G.652) is actively aligned with respect to this embedded fiber using a manual or semi-automatic routine as described below. A certain gap is maintained between both fibers which is filled with a photocurable resin (Norland Optical NOA68). The gap was set at 50 µm since a good uniformity of the fabricated SWW for this length and a decreasing quality for longer structures was observed. Finally, 405 nm illumination from a laser diode is launched (20 µW total power, 30s) from the external fiber into the resin locally forming an SWW from the tip of that fiber. At the same time, a flood UV exposure of the remaining resin is performed (broadband exposure using a mercury lamp, 30 s at 5 mW/cm^2). In principle, only a low-cost laser diode and UV-lamp are required for this process, but by making use of an extra splitter, the optical loss of the SWW can be monitored in real time during fabrication, see Fig. 2. In case the embedded fiber has a connector on the other side (which was ensured during the optimization phase), an insertion loss measurement (in transmission) can be performed using a source (e.g. a pigtailed superluminescent light-emitting diode (SLED)) and detector (e.g. a pigtailed photodiode). As explained below, for connecting real sensors without connectors, the quality of the connection can be evaluated by monitoring the reflection spectrum of the embedded fiber sensor using an optical spectrum analyzer (OSA) or commercial interrogator instead of the measurement in transmission. The setup used and illustrated in Fig. 2 allows monitoring both in transmission and reflection.

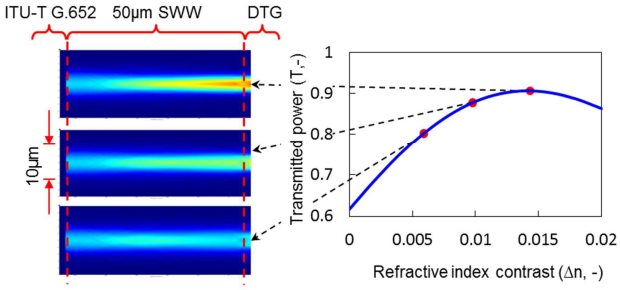

Fig. 3. Simulated fraction of transmitted power between an ITU-T G.652 fiber-SWW (50 µm long)-DTG fiber connection as a function of the refractive index contrast in the SWW ($\Delta n = RI_{core}-RI_{clad}$). The 2D color plots show the power distribution in a longitudinal cross-section in arbitrary units.

The key parameter for achieving a low-loss connection is the refractive index (RI) profile of the SWW which depends on the material used (in this case NOA68 from Norland Products) and the fabrication parameters. Previous work reported the graded-index nature of the resulting SWWs and a corresponding empirical model [7] which is used herein to obtain the ideal SWW RI profile. Using this model, the fraction of power (T, at λ = 1550 nm) transmitted through a 50 µm long SWW section situated between an ITU-T G.652 and DTG fiber was simulated (as a function of the RI contrast of the SWW while keeping the diameter constant) using Finite Difference Time Domain simulations. The RI contrast Δn of the graded-index SWW was defined as the difference of the RI at the center of the waveguide (RI_{core}) and the RI far away from the center (RI_{clad}).

III. Results and Discussion

For an RI contrast of 0.006, the SWW shows the same mode field diameter (MFD) as in an ITU-T G.652 fiber which can be verified by observing that the power distribution (Fig. 3) does not change significantly when the mode propagates from the ITU-T G.652 fiber into the SWW. The SWW acts as an almost perfect extension of this fiber and therefore, this case is similar to the situation in which both dissimilar fibers are directly butt-coupled. However, this leads to a significant loss of almost 1 dB (T = 80 %) because of the different fiber MFDs. Further increasing the RI contrast decreases the diameter of the mode while traveling through the 50 µm long SWW section, thereby increasingly approaching the MFD of

the DTG fiber at the SWW-DTG fiber interface. An optimum transmission (T = 90.7 %, 0.42 dB loss) is reached for an RI contrast of 0.014. It has to be mentioned that the theoretical transmission can further be improved up to 94.4 % by using a 90 µm long SWW, however at the expense of a narrower maximum of the characteristic graph shown in Fig. 3 and a reduced quality of the fabricated SWW structures.

To approach these theoretically predicted transmission values, the SWW fabrication parameters (illumination power and time) were optimized by evaluating the transmitted power during fabrication, using the setup shown in Fig. 2. The maximum transmission for a 50 µm long SWW was achieved for 30 s illumination time using the laser diode power at 20 µW (measured at the tip of the ITU-T G.652 fiber) and a simultaneous flood UV power of 5 mW/cm^2. The corresponding insertion loss signature as a function of illumination time is plotted in Fig. 4 (only the first 24 seconds are shown due to memory limitations of the recording hardware). The reference for these measurements was the transmitted power between the 2 perfectly aligned fibers at nearly 0 µm separation, with (index matching) uncured NOA68 material in between (direct butt coupling). The insertion loss of nearly 1.5 dB at t = 0 s therefore corresponds to the case of 50 µm bulk uncured NOA68 between both fibers. Then, when the illumination process is started, the insertion loss rapidly decreases, proving the formation of an SWW. Since the energy density of the 405 nm illumination launched through the fiber core is much higher than that of the flood exposure, the SWW 'core' is formed first, and is initially surrounded by a liquid, uncured cladding. This leads to a sufficiently high RI contrast and therefore also low insertion loss as expected from the simulation results shown in Fig. 3. Note that the graph drops well below 0 dB, i.e. the presence of the SWW leads to lower insertion losses compared to the reference (butt-coupling) thereby proving its function as mode size converter. Unfortunately, in a later phase (t > 10 s), the loss increases again. The reason is that the flood UV exposure is starting to polymerize the bulk material leading to a higher refractive index of the cladding, thereby reducing the RI contrast with the already formed core. Obviously, this cannot be avoided since the polymerization cannot be stopped and the amount of refractive index contrast upon final polymerization is limited when using a one-polymer approach. Alternatively, a two-polymer approach could be used in which the uncured cladding is substituted by another polymer, thereby allowing larger RI contrasts [7]. However, this requires a developing step (removal of the cladding), which is not desired. Nevertheless, even if the minimum theoretical loss cannot be achieved in reality with NOA68, the final insertion loss after 30 s illumination is still 0.5 dB lower than the case of direct butt-coupling (i.e. the reference value). Furthermore, the use of an intermediate SWW allows greater connection flexibility. For example, in case the embedded fiber is not cut perpendicularly, the free space region between its end-face and that of the external fiber can be bridged by the SWW.

In a real application, there will be no connector on the embedded fiber and therefore the connection quality needs to be validated based on the reflected signal from the Bragg grating sensor. Fig. 5 shows the evolution (throughout the connection process) of this signal, recorded through the external fiber. After forming the SWW, the insertion loss between the 2 fibers at 50 µm separation decreases significantly and the final loss is lower than the reference value, similarly as previously discussed for the measurements in transmission. The noise level at around -30 dB mainly originates from the parasitic reflections at the end-face of the embedded fiber. This noise level is already fairly low owing to the NOA68 material between both fibers, acting as index matching material. If needed, it can further be reduced by polishing the embedded fiber under an angle, however this is not always easy to achieve. In any case, the achieved signal-to-noise ratio and peak reflectivity allows peak tracking using commercial interrogators without any difficulties.

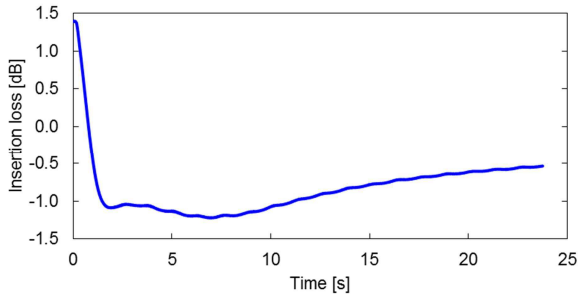

Fig. 4. Insertion loss through an ITU-T G.652 - 50 µm long SWW - DTG fiber connection during SWW fabrication compared to the reference (fibers at 0 µm separation, with uncured NOA68 material in between).

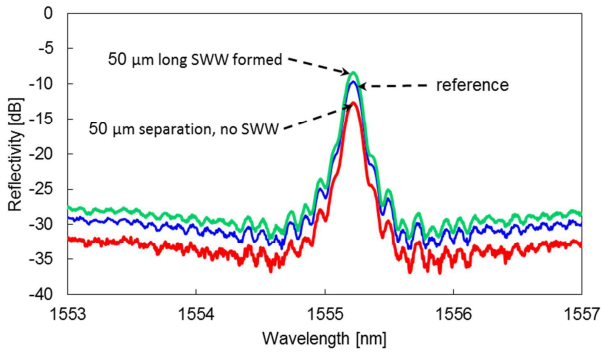

Fig. 5. Reflection spectrum of the embedded DTG fiber sensor recorded at different stages during the connection process.

The discussion above deals with creating a low-loss connection between an embedded fiber and external fiber once both have been aligned. In most cases this alignment step itself is also not trivial when the embedded fiber does not have a connector (e.g. when trimming of the edges is applied after composite production). Fine-tuning of the alignment can be performed by maximizing the peak in the sensor reflection spectrum (cfr. Fig. 5), but before this is possible, the initial coarse position of the fiber needs to be determined. This can be achieved by imaging the cross-section using a camera, but it was found that the embedded fiber was almost not visible when looking with a camera from an angle. Looking under an angle is needed because the holder with the external fiber is

blocking the camera from perpendicularly imaging the cross-section. However, the presence of this external fiber can be used to our advantage for recording the reflection signature of the composite cross-section at the embedded fiber location using only a slight modification of the setup shown in Fig. 2. This signature will reveal the fiber location owing to the difference in reflectivity between the silica fiber and the composite material. To this end, the 1550 nm detector was connected at port 3 of the circulator instead of the OSA and as such the amount of reflected power can be determined. Using a simple script, the external fiber mounted on a motorized stage (Thorlabs Nanomax MAX606) was scanned over the composite cross-section of interest and a reflection measurement was performed at regular intervals. This then results in a characteristic reflection signature as shown in Fig. 6 for the case of a 125 µm diameter silica fiber embedded in a CFRP composite. Note that even the Ormocer® fiber coating can be discerned in this signature. For this measurement, the separation between the scanning fiber and composite was kept fixed at 50 µm and the scanning resolution in both directions parallel to the cross-section was 5 µm. The contours of the fiber can clearly be observed and can be used for coarse positioning of the external fiber after which fine alignment based on the reflection spectrum can be performed. This technique was also validated for locating a sensor fiber embedded inside GFRP composites, however, the difference in reflectivity between the silica fiber and GFRP composite was found lower.

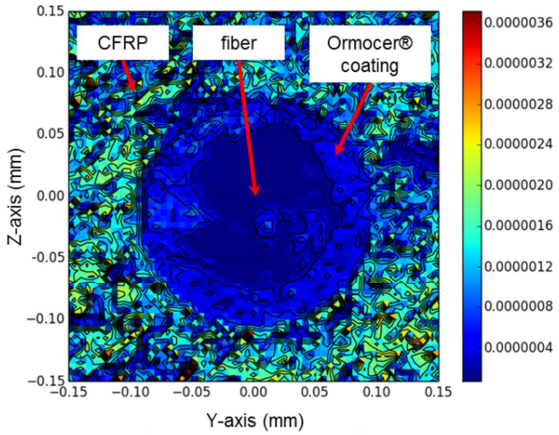

Fig. 6. Reflection signature (λ = 1550 nm) at the cross-section of a 125 µm diameter silica DTG fiber with Ormocer® coating embedded in a carbon fiber reinforced polymer composite. The scan resolution was 5 µm and the color scale represents reflected power (arbitrary units).

The suitability of the presented connection technology for application in the composite industry was further demonstrated by implementing a prototype connector housing which reinforces the optical connection while at the same time providing strain relief for the external fiber. A first version of this prototype was 3D-printed in a fiber reinforced plastic and is shown in Fig. 7, where it is attached to a CFRP and GFRP composite test specimen.

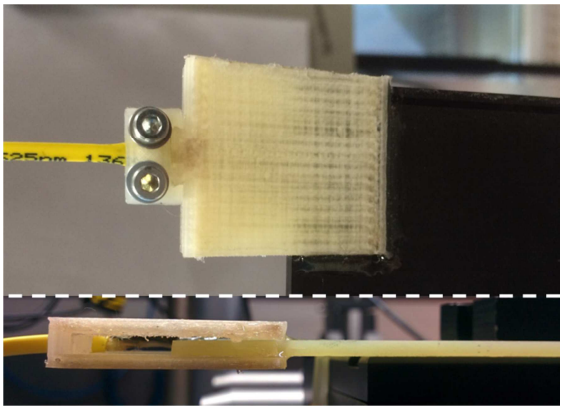

Fig. 7. 3D-printed prototype connector including strain relief for mechanical robustness. The top image shows the connector attached to a CFRP seen from below and the bottom image shows the connector attached to a GFPR composite seen from the side.

IV. Conclusions

A new concept for connecting an embedded optical fiber which does not require special preparation steps was discussed and illustrated for the case of Bragg grating fiber sensors (DTG type) embedded in fiber reinforced polymer composites. Making use of an intermediate SWW, it is possible to implement a mode size converter between the embedded (DTG type) and external fiber (ITU-T G.652) which have a different NA. Although the theoretical minimum connection loss could not be achieved with the available SWW materials used in this work, it was shown that a high-quality grating sensor signal was achieved which could be tracked with a commercial interrogator. The advantage of this connection technology is that it can be applied afterwards, so that optical fiber sensors (without connectors) can be integrated in complex composite structures without needing to adapt the production process or mold.

References

[1] D. Kinet, P. Mégret, K. Goossen, L. Qiu, D. Heider, and C. Caucheteur, "Fiber Bragg Grating Sensors toward Structural Health Monitoring in Composite Materials: Challenges and Solutions," *Sensors*, vol. 14, p. 7394, 2014.

[2] G. Luyckx, E. Voet, N. Lammens, and J. Degrieck, "Strain Measurements of Composite Laminates with Embedded Fibre Bragg Gratings: Criticism and Opportunities for Research," *Sensors*, vol. 11, p. 384, 2011.

[3] H. K. Kang, J. W. Park, C. Y. Ryu, C. S. Hong, and C. G. Kim, "Development of fibre optic ingress/egress methods for smart composite structures," *Smart Mater. Struct.*, vol. 9, p. 149, 2000.

[4] S. Anders, "Manufacturing technique for embedding detachable fiber-optic connections in aircraft composite components," *Smart Mater. Struct.*, vol. 9, p. 855, 2000.

[5] A. K. Green and E. Shafir, "Termination and connection methods for optical fibres embedded in aerospace composite components," *Smart Mater. Struct.*, vol. 8, p. 269, 1999.

[6] M. Kagami, T. Yamashita, and H. Ito, "Light-induced self-written three-dimensional optical waveguide," *Applied Physics Letters*, vol. 79, pp. 1079-1081, 2001.

[7] J. Missinne, S. Beri, M. Dash, S. K. Samal, P. Dubruel, J. Watté, *et al.*, "Curing kinetics of step-index and graded-index single mode polymer self-written waveguides," *Optical Materials Express*, vol. 4, p. 1324, 2014/07/01 2014.